CONFERENCE PRE-PRINT

ION AND ELECTRON HEATING VIA MAGNETIC RECONNECTION DURING MERGING/COMPRESSION PLASMA STARTUP IN ST40

H. TANABE, R. SOMEYA, T. AHMADI
Graduate school of frontier sciences, university of Tokyo
Bunkyo-ku/Tokyo, Japan
Email: tanabe@k.u-tokyo.ac.jp

M. GRYAZNEVICH, D. OSIN, H. V. WILLETT, H. LOWE, H. BOHLIN, T. O'GORMAN, J. WOOD, A. RENGLE, S. MCNAMARA, P. BUXTON, O. ASUNTA
Tokamak Energy Ltd.
Milton Park, Oxfordshire, United Kingdom

Abstract

Here we report the latest report on the high field application of merging/compression (M/C) and reconnection plasma startup in the ST40 spherical tokamak using 96CH 2D ion Doppler tomography and 30CH Thomson scattering diagnostics which were installed in the last 2 years. The new findings and achievements in the last 2 years are summarized as follows: (i) the new 2D 96CH ion Doppler tomography clearly revealed ion heating on the trajectory/downstream of reconnection outflow jet and its confinement/transport process. (ii) Electron density also increases at the same region, while electrons are heated around the X-point (or magnetic axis) and electron temperature profile forms a peaked profile. (iii) Quasi-steady sustainment/confinement of M/C startup plasma current and ion temperature has been demonstrated. (iv) Based on series of M/C experiments, $I_p \propto I_{MC}$ scaling was upscaled to $I_p \sim 600$kA. (v) Full pressure profile measurement leads to the evaluation of energy conversion ratio of the dissipated magnetic energy of reconnecting field B_{rec} and it was found that ~ 30% of released magnetic energy was converted to ion thermal energy and the previously demonstrated $\Delta T_i \propto B_{rec}^2$ scaling has successfully been upgraded to $\Delta U_i = 1.5(\Delta n_e \kappa_B T_i) \propto B_{rec}^2$ scaling ($\Delta U_i \sim 10$kJ/m^3 which was 10 times higher than the record in MAST was explored in ST40) for the first time.

1. INTRODUCTION

Achieving high-performance plasma startup and ramp-up with minimal solenoid flux consumption is a key challenge in spherical tokamak (ST) research [1-3]. Due to the limited space in the centre stack, a critical design trade-off must be addressed when constructing a new device: higher toroidal field (B_t) with reduced space for the central solenoid (CS), or lower B_t with more room for the CS. In the last 3 decades of ST research, various central solenoid (CS)-free startup scenarios were proposed/tested to reduce the reliance on CS to change the optimum point of the design trade-off such as merging compression (M/C) [4], local helicity injection (LHI) [5], electron Bernstein wave (EBW) plasma startup [6] and so on. M/C and LHI explored high beta records [7, 8, 9] and H-mode performance [10] in mega-ampere (MA) scale experiments [1, 4, 11], while the latter RF method explores long pulse steady scenario which has longer duration time than 100ms [1, 3]. In addition to those achievements of CS-free plasma formation methods, M/C startup is also known to have the additional advantage of MW–GW scale impulsive plasma heating during the merging phase through energy conversion via magnetic reconnection [12].

Magnetic reconnection is the underlying physics of the additional heating performance of merging/compression. Through the rearrangement of the topology of anti-parallel magnetic field lines [13, 14], magnetic energy is converted to kinetic/thermal energy of plasmas, and it leads to particle acceleration and heating in proportion to the square of reconnecting magnetic field component B_{rec} ($\Delta T_i \propto B_{rec}^2$) [15]. Magnetic reconnection is observed in many fusion, laboratory and astrophysical plasmas such as sawtooth crashes [16], merging compression of two flux tubes [4, 15], geomagnetic substorms in the Earth's magnetosphere and solar flares [13, 14, 17]. In the 1990's, the application of reconnection heating was pioneered in TS-3 and START with MW-GW scale significant ion heating by merging two plasma rings (merging/compression) [1, 4, 8, 11], MAST achieved the first demonstration of reconnection heating in keV regime in the last two decades [18] and ST40 is now on the way of demonstrating further high performance [19]. In the last three decades, heating mechanism of magnetic reconnection was investigated in a number of experiments: TS-3 [15], MRX [20], SSX [21], VTF [22], TS-4 [23], UTST (TS-5) [24], C-2U [25], MAST [26], TS-6 (TS-3U) [27] and ST40 [28]. For those experiments, the following common characteristics have been reported: (i) magnetic reconnection heats ions downstream and electrons around the *X*-point where magnetic field lines reconnect [15]; (ii) ions are heated by outflow dissipation downstream [29] while electrons gain energy mostly by resistive dissipation of current sheet around the *X*-point [30]; (iii) ions typically

gain most of heating energy, and electron heating is small [31] (global ion heating and localized electron heating around the *X*-point); and (iv) the heating performance simply depends on the released energy of reconnecting field B_{rec} (poloidal field B_p for toroidal plasmas) as in $\Delta T_i \propto B_{rec}^2$ scaling demonstration [15, 30]. In addition to those common/fundamental characteristics of reconnection heating, reconnection originated fine structure was found in MAST [26, 32], UTST [33] and TS-6 [27] experiments, satellite observations [34] and PIC simulation [35]. When high guide field B_g is applied (toroidal field B_t), highly localized hot spot of electron heating is around the *X*-point in a smaller scale than ion skin depth c/ω_{pi} [26, 36] and high T_i region also forms fine structure in the diffusion region as well as downstream [37, 38]. Ion-electron decoupling via non-MHD activity leads to quadrupole potential structure [39] and poloidally tilted ion temperature profile was found in TS-3U by mass ratio scanning experiment which changes ion skin depth and gyro radius [27]. In TS-6, post-MAST experiment with further high-resolution diagnostics [40, 41] leads to the finding of positive potential side ion heating via parallel acceleration and poloidally ring-like global structure formation by parallel heat transport [42].

Application of the impulsive plasma heating by magnetic reconnection, merging/compression (M/C), was first pioneered in START [43] and TS-3 [8] in 1990's with the well-known high beta plasma performance $\beta > 40\%$. MAST demonstrated first 1keV heating [30] by M/C in 2000's and achieved longer pulse duration time than 100ms in fully CS-free (M/C only) scenarios by suppressing current decay rate with the high temperature startup [32]. In 2010's, the understanding of the reconnection heating physics with $\Delta T_i \propto B_{rec}^2 \propto B_p^2$ scaling provides the design criteria of upgraded M/C experiments [32, 44, 45]. The idea leads to the design of high field MC coils in ST40 and $\Delta T_i \sim$ 2keV was demonstrated in 2018 with the fully CS-free operation. From 2019, M/C-solenoid hybrid scenario and auxiliary heating by NBIs have been explored [46] and the world first achievement of 100MK spherical tokamak in 2022 is now widely known in public [47]. However, nevertheless of those achievements, previous publication mostly relies on 0-D measurement such as line-average density/temperature and detailed reports on M/C process with proper profile measurement has never been published. As a major progress in the last 3 years, 30CH Thomson scattering measurement and 32CH 1D Doppler tomography [48, 49] was installed in 2023. Next year in 2024, the U-Tokyo Doppler tomography was upgraded to a 96CH 2D imaging system [50]. In this paper, here we report the detailed heating process of magnetic reconnection during M/C plasma startup in ST40.

2. MERGING/COMPRESSION PLASMA STARTUP IN ST40

Figure 1 shows an example of merging/compression (M/C) application scenario in ST40 with full waveform of all PF coils (MC (11 turns), PSH (8 turns), BVU (8 turns), BVL (16 turns) and DIV (28 turns) and solenoid (SOL) coils [51]). As illustrated by fast camera images, two plasma rings are formed at the top and the bottom of the device at t = 0ms and those rings merge together at t = 10ms. During this process, plasma current quickly increases up to I_p = 0.6MA. Before the beginning of solenoid ramp as shown in the light blue colour (I_{SOL}), MC and PSH coils are mainly used for the major driving coils of M/C. The induction of I_{MC} is the major driving current of merging/compression and the negative I_{PSH} assists the merging process by driving plasma inflow during magnetic reconnection. Central solenoid is used for additional plasma current ramp up and sustainment of flat-top I_p.

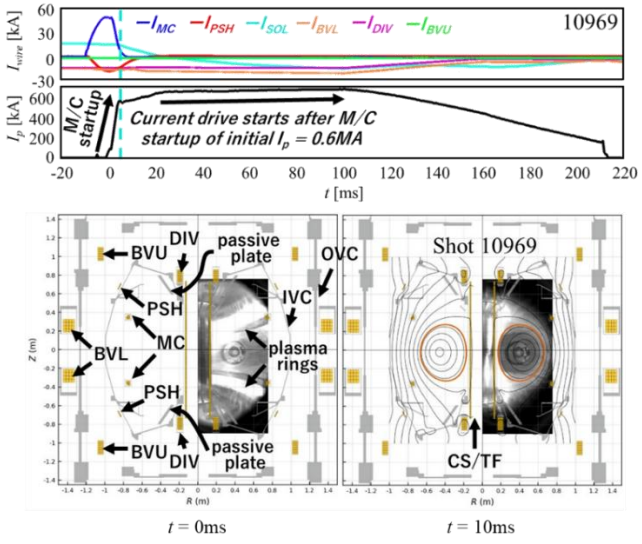

FIG. 1. Full waveform of high-I_p plasma scenario on 10969 and merging/compression plasma startup in ST40

3. ION AND ELECTRON HEATING DURING MERGING/COMPRESSION IN ST40

Figure 2 shows more detailed time evolution of fast camera images during M/C (major radius $R_0 \sim 0.4$m and I_p = 0.35MA) and 2D ion temperature profile T_i measured by 96CH 2D ion Doppler tomography which was shipped from the university of Tokyo (16CH (radial: 250mm < r < 740mm)×6 vertical arrays (z = - 25.0mm, -7.5mm, 7.5mm, 25.0mm, 42.5mm and 60.0mm)) [50]. As in the fast camera images, two plasma rings are initially formed around MC coils. Around t = 7ms, vertically pushed plasmas are disconnected from MC coils and merging/reconnection occurs. Reference flux profile from EFIT reconstruction at t = 10ms is also shown ($R_0 \sim$ 0.4m). In ST40, direct measurement of poloidal flux profile is not available but the measured 2D ion temperature profile at t = 7ms suggests that X-point/current-sheet is located around (r, z) ~ (0.4m, 0.0m) and reconnection outflow propagates toward (r, z) ~ (0.3m, 0.0m) and (0.5m, 0.0m) to form characteristic double-peak structure based on outflow heating mechanism. The thickness of the current sheet-like structure is thinner than ion skin depth (50mm < c/ω_{pi} < 100mm) and MAST-like fine structure in the two-fluid scale is detected [52]. At t = 8ms, the high T_i region propagates toward vertically mostly by parallel heat conduction ($\kappa^i_{//}/\kappa^i_{\perp} \sim 2(\omega_{ci}\tau_{ii})^2 >> 1$) [27, 42, 50, 52] and ions are globally heated inside the closed flux surface at t = 9ms.

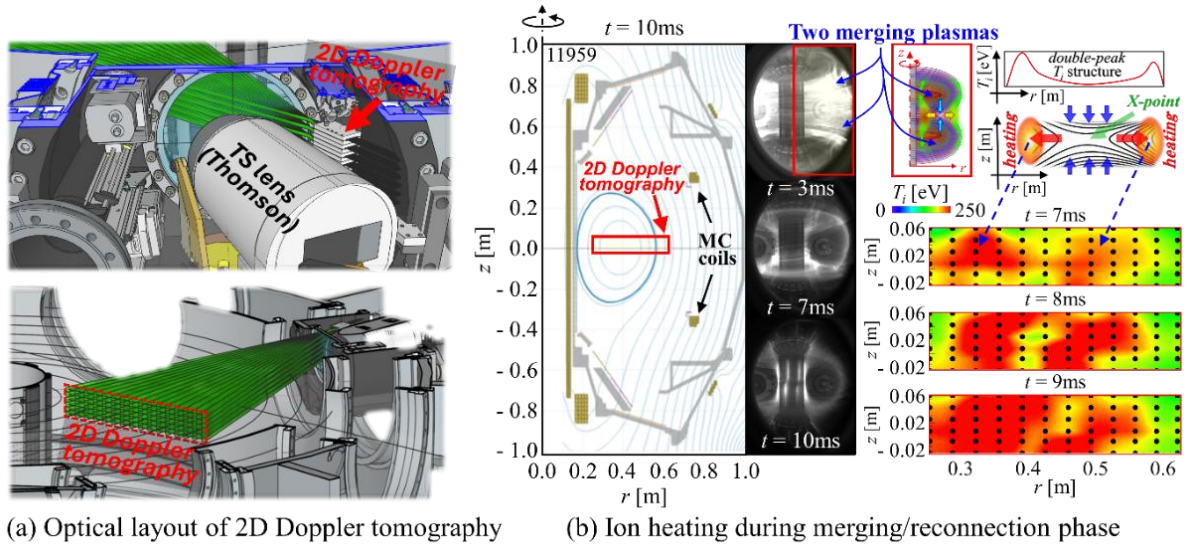

FIG. 2. Time evolution of visible light emission (fast camera) and 2D ion temperature (T_i) profile (96CH ion Doppler tomography) during merging/reconnection phase in ST40 (major radius R_0 is ~ 0.4m as in EFIT at t = 10ms).

Figure 3 shows a synchronized measurement with 30CH Thomson and ion Doppler tomography: electron temperature T_e, density n_e and ion temperature T_i profiles at t = 7ms (FIG. 3 left) and t = 8ms (FIG. 3 middle), the characteristics time frames during reconnection heating ($I_p \sim$ 0.4MA and $R_0 \sim$ 0.5m). Figure 3 (right) illustrates more detailed time evolution of T_e, electron pressure p_e and energy increment $\Delta U_e/\Delta t = 1.5(\Delta n_e \kappa_B T_e/\Delta t)$. T_e typically increases at the central region ($r \sim$ 0.5m) where X-point is expected to exist, while n_e and T_i forms broad/hollow profile through outflow acceleration/heating [26]. As shown in FIG. 3 right, T_e is initially tens of eV before the reconnection heating starts at t = 4ms and 5ms but it starts to increase around t = 7ms when the merging plasmas are detached from MC coils. At t = 8ms, T_e and p_e forms the characteristic peaked structure at the central region where current sheet dissipation and parallel acceleration occur, and then the peak T_e and p_e become wider at t = 9ms. Between t = 7ms and 8ms, $\Delta U_e/\Delta t$ forms peaked structure in 3MW/m^3. Then, between t = 8ms and 9ms, collisional coupling between electrons and ions also supplies additional electron heating (~ 2MW/m^3) at r = 0.40m and 0.55m where T_i profile forms characteristic double-peak. Finally bulk electrons and ions are both heated through merging/compression startup.

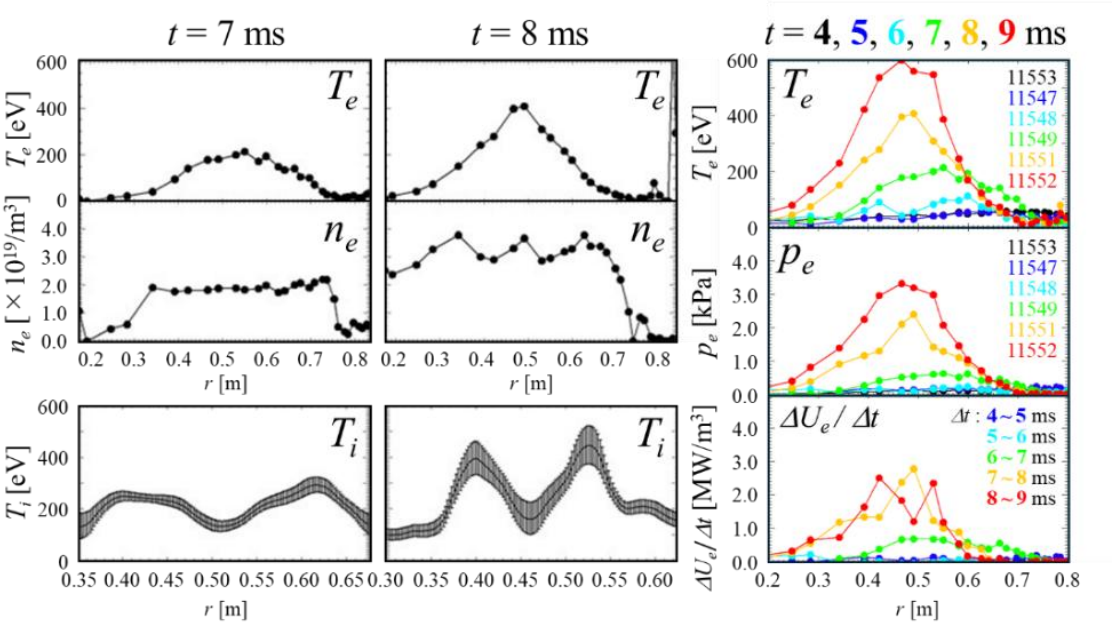

FIG. 3. Electron and ion heating during merging/reconnection phase. T_e typically forms peaked profile around the central region, while n_e and T_i forms broad/hollow profile. Characteristic energy deposition is observed around X-point ($r \sim 0.5$m) where current sheet dissipation occurs and the outflow region ($r \sim 0.40$m and 0.55m) via ion-electron energy relaxation.

Figure 4 shows time evolution of I_{MC} and I_p (FIG.4 (a)), supporting scaling of I_p formation as a function of I_{MC} (FIG.4 (b)) and time evolution of ion temperature profile T_i (FIG.4 (c)) in a longer time scale when I_p = 0.4MA and $R_0 \sim 0.4$m. The initial plasma current I_p linearly increases as a function of I_{MC} ($I_p \propto I_{MC} \times N$) and the startup I_p level can be freely selected: maximum I_{MC} is used for $I_p \sim 0.6$MA startup scenario in FIG.1 and $I_{MC} \times N$ = 400kA·turn is used for the $I_p \sim 0.4$MA scenario on 12405. Merging/reconnection heating of ions lasts until t = 10 ~ 12ms with double-peak ion heating structure and T_i at the central region also increases after that through the collisional coupling between electrons. Finally ~1keV bulk T_i is formed and auxiliary heating starts after that as demonstrated in the 10keV scenario on 10009 [47].

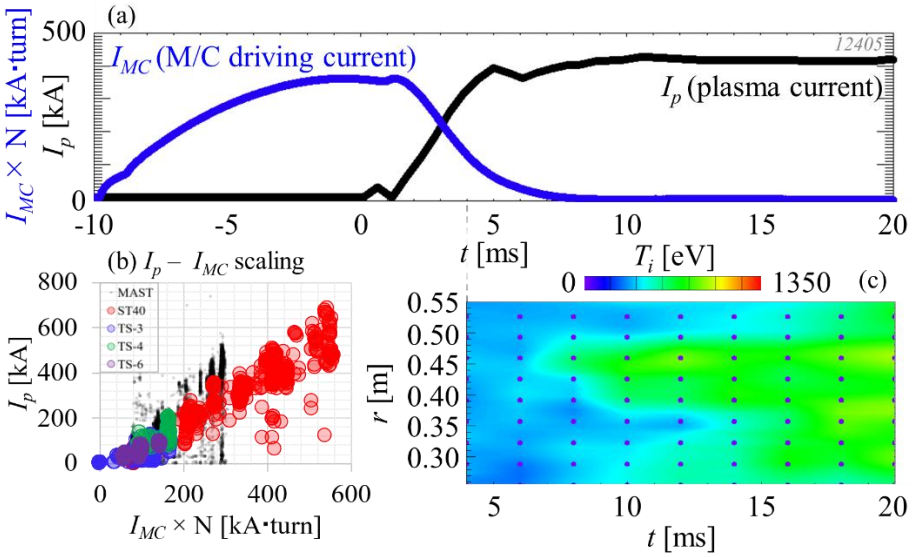

FIG. 4. Demonstration of sustainment/connection of M/C startup parameters (I_p and T_i) to a quasi-steady plasma scenario and M/C startup performance summary (I_p – I_{MC} scaling). M/C startup heat ions globally in ~1keV with $I_p \sim 0.4$MA.

Figure 5 illustrates the evaluation of the ion thermal energy increment $\Delta U_i = 1.5(\Delta n_e \kappa_B T_i)$ via merging/reconnection heating as a function of the reconnecting field $B_{rec} \sim B_p$ which is in proportion to plasma current I_p. Because the source of reconnection heating is the released magnetic energy of reconnection field $B_{rec}^2/2\mu_0$, ΔU_i via reconnection heating satisfies $\Delta U_i \propto B_{rec}^2 \propto I_p^2$. ΔU_i is in the order of 1kJ/m^3 in MAST with $B_{rec} \sim 0.1$T and $\Delta U_i \sim 9$kJ/m^3 in ST40 with $B_{rec} \sim 0.3$T. The upgrade of B_{rec}^2 scaling from $\Delta T_i \propto B_{rec}^2$ to $\Delta U_i \propto B_{rec}^2$ the assessment of energy conversion efficiency: roughly ~ 30% of magnetic energy is converted to ion thermal energy. In the millisecond time scale M/C experiments in ST40 and MAST, electron temperature also documented similar temperature to ions through ion-electron energy relaxation and totally more than 50% of magnetic energy is converted to plasma thermal energy ($\Delta U_i + \Delta U_e$) in the merging/compression startup process.

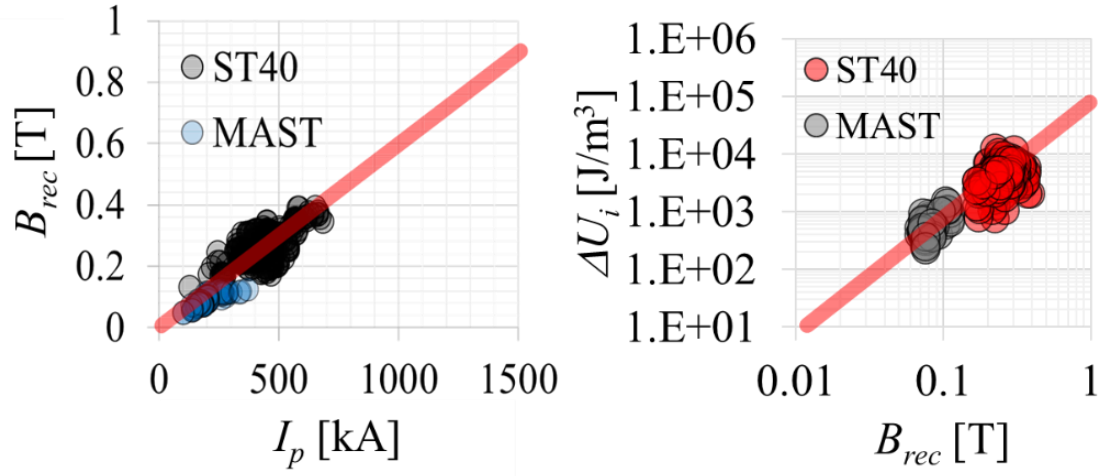

FIG. 5. Ion heating scaling $\Delta U_i \propto B_{rec}^2 \propto I_p^2$: 30% of released magnetic energy is converted to ion thermal energy ΔU_i.

4. CONCLUSION

First detailed investigation of reconnection heating process during M/C startup in ST40 has been conducted and the rapid plasma heating/startup process has successfully been revealed using the new 2D 96CH Doppler tomography and the 30CH Thomson scattering diagnostics. The high field application of M/C heating scenario in ST40 successfully demonstrated to form ~ 10 times higher pressure than the previous record in MAST based on B_{rec}^2 scaling and its sustainment/connection to steady scenario. The new findings from this research is summarized as follows:

- M/C startup I_p level is nearly same as the MC driving coil current: $I_p \propto I_{MC} \times$ N.
- Magnetic reconnection heats ions on the trajectory of reconnection outflow jet whose thickness is thinner than ion skin depth and more in the downstream region to form double-peak T_i structure.
- Under the influence of high toroidal guide field B_t, perpendicular heat conduction is negligibly small ($\kappa^i_{//}/\kappa^i_{\perp} \sim 2(\omega_{ci}\tau_{ii})^2 >> 1$) and poloidally ring-like hollow ion temperature profile is formed during ion heating/transport phase. Semi-steady confinement of the M/C startup high T_i has been demonstrated.
- Electron temperature initially increases around X-point where current sheet dissipation and parallel electric acceleration occurs and T_e profile forms peaked structure.
- Bulk electrons are also heated by ion-electron energy relaxation in the millisecond time scale and the characteristic peaked structure gets broader after merging.
- Ion heating scaling $\Delta T_i \propto B_{rec}^2$ has been upgraded to $\Delta U_i \propto B_{rec}^2$ in collaboration with Thomson scattering measurement of n_e and it was found that 30% of magnetic energy is converted ion thermal energy

Based on those findings, ion heating in 10keV is potentially possible if B_p = 0.6T and $n_e = 2\times10^{19}/m^3$ based on the upgraded reconnection heating scaling $\Delta U_i \propto B_{rec}^2$. For example, it is possible if higher I_{MC} startup scenario which leads to I_p ~ 1MA and B_p ~ 0.6T with $I_{MC}\times$ N ~ 1MA·turn is available in ST40. The further upgraded design criteria to enable direct burning plasma formation by M/C has clearly been established with the upgraded scaling.

ACKNOWLEDGEMENTS

This work was supported by Grants-in-Aid for Scientific Research 22H01193, 23K22464, 23KF0194 and 23KK0246, and NIFS Collaboration Research programs NIFS24KIIS008 and NIFS25KIIM005.

REFERENCES

[1] Raman, R. and Shevchenko, V.F., Solenoid-free plasma start-up in spherical tokamaks, Plasma Phys. Control. Fusion (2014) **56** 103001

[2] Costley, A.E. and McNamara, S.A.M., Fusion performance of spherical and conventional tokamaks: implications for compact pilot plants and reactors, Plasma Phys. Control. Fusion (2021) **63** 035005

[3] Shevchenko, V.F., O'Brien, M.R., Taylor, D., Saveliev, A.N. and MAST team, Electron Bernstein wave assisted plasma current start-up in MAST, Nucl. Fusion (2010) **50** 022004

[4] Gryaznevich, M. and Sykes, A., Merging-compression formation of high temperature tokamak plasma, Nucl. Fusion (2017) **57** 072003

[5] Bongard, M.W., Bodner, G.M., Burke, M.G., Fonck, R.J., Pachicano, J.L., Perry, J.M., Pierren, C., Reusch, J.A., Rhodes, A.T., Richner, N.J., Sanchez, C.R., Schaefer, C.E. and Weberski, J.D., Advancing local helicity injection for non-solenoidal tokamak startup, Nucl. Fusion (2019) **59** 076003

[6] Shevchenko, V.F., O'Brien, M.R., Taylor, D., Saveliev, A.N. and MAST Team, Electron Bernstein wave assisted plasma current start-up in MAST, Nucl. Fusion (2010) **50** 022004

[7] Gryaznevich, M. et al, Achievement of record β in the START spherical tokamak, Phys. Rev. Lett. (1998) **80** 3972

[8] Ono, Y., Kimura, T., Kawamori, E., Murata, Y., Miyazaki, S., Ueda, Y., Inomoto, M., Balandin, A.L. and Katsurai, M., High-beta characteristics of first and second-stable spherical tokamaks in reconnection heating experiments of TS-3, Nucl. Fusion (2003) **43** 789

[9] Sykes, A. et al, H-Mode Operation in the START Spherical Tokamak, Phys. Rev. Lett. (2000) **84**, 495

[10] Schlossberg, D.J., Bodner, G.M., Bongard, M.W., Burke M.G., Fonck R.J., Perry J.M. and Reusch J.A., Noninductively Driven Tokamak Plasmas at Near-Unity Toroidal Beta, Phys. Rev. Lett. (2017) **119**, 035001

[11] Kirk, A. et al, Overview of recent physics results from MAST, Nucl. Fusion (2017) **57** 102007

[12] Ono, Y., Yamada, M., Akao, T., Tajima, T. and Matsumoto, R., Ion acceleration and direct ion heating in three-component magnetic reconnection, Phys. Rev. Lett. (1996) **76** 3328

[13] Zweibel, E.G. and Yamada, M., Magnetic reconnection in astrophysical and laboratory plasmas, Annu. Rev. Astron. Astrophys. (2009) **47** 291

[14] Yamada, M., Kulsrud, R. and Ji, H., Magnetic reconnection, Rev. Mod. Phys. (2010) **82** 603

[15] Ono, Y. et al, Ion and electron heating characteristics of magnetic reconnection in a two flux loop merging experiment, Phys. Rev. Lett. (2011) **107** 185001

[16] Chapman, I.T., Scannell, R., Cooper, W.A., Graves, J.P., Hastie, R.J., Naylor, G. and Zocco, A., Magnetic Reconnection Triggering Magnetohydrodynamic Instabilities during a Sawtooth Crash in a Tokamak Plasma, Phys. Rev. Lett. (2010) **105**, 255002

[17] Masuda, S., Kosugi, T., Hara, H. et al, A loop-top hard X-ray source in a compact solar flare as evidence for magnetic reconnection. Nature (1994) **371** 495

[18] Ono, Y. et al, Ion and electron heating characteristics of magnetic reconnection in tokamak plasma merging experiments, Plasma Phys. Control. Fusion (2012) **54** 124039

[19] Gryaznevich, M. and Asunta, O., Overview and status construction of ST40 Fusion Eng. Des. (2017) **123** 177

[20] Yamada, M., Ji, H., Hsu, S., Carter, T., Kulsrud, R., Bretz, N., Jobes, F., Ono, Y. and Perkins, F., Study of driven magnetic reconnection in a laboratory plasma, Phys. Plasmas (1997) **4** 1936

[21] Brown, M., Experimental studies of magnetic reconnection, Phys. Plasmas (1999) **6** 1717

[22] Egedal, J., Fasoli, A., Porkolab, M. and Tarkowski, D., Plasma generation and confinement in a toroidal magnetic cusp, Rev. Sci. Instrum. (2000) **71** 3351

[23] Tanabe, H., Oka, H., Annoura, M., Kuwahata, A., Kadowaki, K., Kaminou, Y., You, S., Balandin, A.L., Inomoto, M. and Ono, Y., Two dimensional imaging measurement of magnetic reconnection outflow in the TS-4 toroidal plasma merging experiment, Plasma Fusion Res. (2013) **8** 2405088
[24] Inomoto, M. et al, Centre-solenoid-free merging start-up of spherical tokamak plasmas in UTST, Nucl. Fusion (2015) **55** 033013
[25] Binderbauer, M.W. et al, Recent breakthroughs on C-2U: Norman's legacy, AIP Conf. Proc. (2016) **1721** 030003
[26] Tanabe, H. et al, Electron and ion heating characteristics during magnetic reconnection in the MAST spherical tokamak, Phys. Rev. Lett. (2015) **115** 215004
[27] Tanabe, H., Cao, Q., Tanaka, H., Ahmadi. T., Akimitsu, M., Sawada, A., Inomoto, M. and Ono Y., Investigation of fine structure formation of guide field reconnection during merging plasma startup of spherical tokamak in TS-3U, Nucl. Fusion (2019) **59** 086041
[28] Gryaznevich, M. and Tokamak Energy team, Faster fusion: ST40, engineering, commissioning, first results, AIP Conference Proceedings (2019) **2179** 020008
[29] Yoo, J. et al, Observation of ion acceleration and heating during collisionless magnetic reconnection in a laboratory, plasma Phys. Rev. Lett. (2013) **110** 215007
[30] Ono, Y. et al, High power heating of magnetic reconnection in merging tokamak experiments, Phys. Plasmas (2015) **22** 055708
[31] Yamada, M. et al, Conversion of magnetic energy in the magnetic reconnection layer of a laboratory plasma, Nat. Commun. (2014) **5** 4774
[32] Tanabe, H. et al, Investigation of merging/reconnection heating during solenoid-free startup of plasmas in the MAST Spherical Tokamak, Nucl. Fusion (2017) **57** 056037
[33] Inomoto, M. et al, Effects of reconnection downstream conditions on electron parallel acceleration during the merging start-up of a spherical tokamak, Nucl. Fusion (2019) **59** 086040
[34] Hara, H., Watanabe, T., Harra, L.K., Culhane, J.L. and Young, P.R., Plasma motions and heating by magnetic reconnection in a 2007 May 19 flare, Astrophys. J. (2011) **741** 107
[35] Inoue, S. et al, Numerical study of energy conversion mechanism of magnetic reconnection in the presence of high guide field, Nucl. Fusion (2015) **55** 083014
[36] Yamada, T. et al, Localized electron heating during magnetic reconnection in MAST, Nucl. Fusion (2016) **56** 106019
[37] Tanabe, H., Cao. Q., Tanaka, H., Ahmadi, T., Akimitsu, M., Sawada, A., Inomoto, M. and Ono, Y., Recent Progress in High Resolution 2D Imaging Measurements of Reconnection Heating during Merging Plasma Startup in TS-3, Plasma and Fusion Res. (2019) **14** 3401110
[38] Tanabe, H. et al, Recent progress of magnetic reconnection research in the MAST spherical tokamak, Phys. Plasmas (2017) **24** 056108
[39] Yamasaki, K. et al, Laboratory study of diffusion region with electron energization during high guide field reconnection, Phys. Plasmas (2015) **22** 101202
[40] Tanaka, H., Ono, Y., Tanabe, H. and Cao. Q, First global Doppler tomography measurement of ion heating of merging tokamak plasmas, IEEJ Trans. FM (2019) **13** 8
[41] Cao, Q., Cai, Y., Akimitsu, M. Xiang, J. Ahmadi, T., Tanaka, H., Tanabe, H.,and Ono, Y., Spontaneous formation of plasmoid during early magnetic reconnection phase of two merging tokamaks, IEEJ Trans. (2020) **15** 1403
[42] Tanabe, H., Tanaka, H., Cao, Q., Cai Y., Akimitsu, Ahmadi. T., A., Cheng, C. Z., Inomoto, M. and Ono Y., Global ion heating/transport during merging spherical tokamak formation, Nucl. Fusion (2021) **61** 106027
[43] Peng, Y.-K. M., The physics of spherical torus plasmas, Phys. Plasmas (2000) **7** 1681
[44] Ono, Y. et al, Reconnection heating experiments and simulations for torus plasma merging start-up, Nucl. Fusion (2019) **59** 076025
[45] Ono Y., et al, Ion heating characteristics of merging spherical tokamak plasmas for burning high-beta plasma formation, Nucl. Fusion (2024) **64** 086020
[46] Gryaznevich, M., TE. Ltd Physics Team and TE. Ltd HTS Team for Tokamak Energy Ltd, Experiments on ST40 at high magnetic field, Nucl. Fusion (2022) **62** 042008
[47] Mcnamara, S. et al, Achievement of ion temperatures in excess of 100 million degrees Kelvin in the compact high-field spherical tokamak ST40, Nucl. Fusion (2023) **63** 054002
[48] Tanabe, H. et al, Two-dimensional ion temperature measurement by application of tomographic reconstruction to Doppler spectroscopy, Nucl. Fusion (2013) **53** 093027

[49] Tanabe, H. et al, Application of tomographic ion Doppler spectroscopy to merging plasma startup in the MAST spherical tokamak, Plasma Fusion Res. (2016) **11** 1302093
[50] Tanabe, H. et al, Ion heating/transport characteristics of the merging startup plasma scenario in the TS-6 spherical tokamak, Nucl. Fusion (2024) **64** 106008
[51] Asunta, O. et al, ST40 data and control, Fusion Engineering and Design (2019) **146** 2194
[52] Browning, P.K. et al, Two-fluid and magnetohydrodynamic modelling of magnetic reconnection in the MAST spherical tokamak and the solar corona, Plasma Phys. Control. Fusion (2016) **58** 014041